doi.org/10.36721/PJPS.2026.39.7.184.1

# Thermo-acoustic and computational studies for the mixture of drug (NSAIDs) and D-mannitol in an aqueous system: Implications for pharmaceutical formulation

**Sumaira Shoukat, Muhammad Asghar Jamal*, Faiz Ahmed and Majid Muneer**
Department of Chemistry, Government College University, Faisalabad, Pakistan

**Abstract**: **Background**: The interactions of non-steroidal anti-inflammatory drugs (NSAIDs) with excipients significantly influence their solubility, stability and bioavailability, and have a significant impact on the therapeutic efficacy of drugs. **Objectives**: The present study explores the molecular interactions between the NSAID and D-mannitol in an aqueous system over the temperature range 293.15 to 313.15 K, using thermo-acoustic and computational techniques. **Methods**: Thermo-acoustic parameters, including apparent and partial molar volume ($\emptyset_v$, $\emptyset_v^\circ$), apparent and partial molar isentropic compressibility ($\emptyset_k, \emptyset_k^\circ$), and transfer partial molar volume ($\Delta_{tr}\emptyset_v^\circ$), etc, were calculated using experimental data of density ($\rho$) and sound velocity ($u$). **Results**: The positive values of partial molar volume and the negative value of partial molar isentropic compressibility indicate the existence of molecular interactions. The positive values of $\Delta tr\emptyset v^\circ$ indicate the existence of ion-hydrophilic and hydrophilic-hydrophilic interactions. Hepler's constant $\left(\frac{\partial^2\emptyset_v^\circ}{\partial T^2}\right)_p$ indicates that Sodium naproxen (Na-NAP) acts as a structure-maker in the presence of D-mannitol in the aqueous solution. In addition to volumetric and acoustic studies, computational work involving HOMO–LUMO analysis, single-point energy calculations, dipole moments, and global reactivity descriptors highlights the stability and reactivity of the interacting species. In the gas phase, the HOMO–LUMO gap decreased significantly (0.29 eV), but it increased in aqueous medium (2.83 eV), suggesting that the complex has stabilized. **Conclusion**: These findings offer a strong foundation for stabilizing drugs through structure-making behaviour, providing a rational basis for developing effective pharmaceutical formulations.

**Keywords**: D-mannitol; DFT; Expansibility; Sodium naproxen; Transfer partial volume

*Submitted on 09-12-2025 – Revised on 03-01-2026 – Accepted on 24-01-2026*

## INTRODUCTION

The primary priority in current therapeutic practice is the development of drug formulations with optimized solubility, stability, and reduced adverse effects. The interactions between drugs and biologically relevant excipients, such as D-mannitol, are crucial for understanding the pharmacodynamics and pharmacokinetic behaviour of the drug. Hydrogen bonding, ion-dipole forces, hydrophobic hydration and electrostatic associations are some examples of these interactions. The nature and strength of these interactions in aqueous media can be effectively understood through physicochemical studies, particularly when the concentrations of the drug and excipients vary (Sharma *et al*., 2017). Understanding the molecular interactions between medications and excipients is crucial for developing stable and effective formulations. Thermo-acoustic measures, such as density and sound velocity, provide sensitive indications about molecular packing, solvation patterns, and structural behaviour within the solution. These findings can be directly related to modern formulation procedures, including rational excipient selection, dosage form optimization, and solution stability prediction. Overall, aqueous-phase studies are crucial to biophysical and medicinal chemistry by revealing mechanisms of intermolecular interactions that may ultimately affect drug performance and formulation design (Lomesh, Bala, Kumar, *et al.*, 2019; Nain, 2019). Non-steroidal anti-inflammatory (NSAIDs) drugs treat pain, inflammation, osteoarthritis, rheumatoid arthritis, and musculoskeletal diseases due to their potent analgesic and anti-inflammatory properties. NSAIDs also prevent heart attacks and colon cancer, mainly acting as a blood vessel-clotting inhibitor. Sodium naproxen (Na-NAP) is derived from propionic acid. Na-NAP is an effective analgesic for several acute pain conditions, including tension headaches, migraines, postpartum and postoperative pain and pain from various gynaecological operations (Filippa and Gasull, 2014; Perlovich *et al*., 2004).

Advanced drug delivery systems, including micelles and nanoparticles, still depend on excipients to maintain structural stability (Chen *et al*., 2019). A common polyhydroxy excipient, D-mannitol, is widely used in the food, chemical, and pharmaceutical industries due to its low caloric content, osmotic activity, and minimal effect on blood glucose levels. (Lomesh *et al*., 2024). It is commonly used to treat elevated intracranial pressure (ICP), to protect the kidneys during cardiac, vascular and renal transplant surgery and to treat rhabdomyolysis. This concurrent use may result in excipient–drug or food–drug interactions, which can change the stability, solubility, or

*Corresponding author: e-mail: asgharjamal@gcuf.edu.pk

absorption of the drug, so it is crucial to comprehend the way drug and D-mannitol interact. The hydroxyl groups of D-mannitol can form hydrogen-bond networks, affecting the hydration structure surrounding the sodium ion and naproxenate anion (Lomesh, Bala, and Nathan, 2019; Sharma *et al.*, 2017). These drug macromolecular interactions provide a thorough understanding of how the drug works, is absorbed, and crosses biological membranes, which is crucial for medical and pharmaceutical chemistry (Dudley, 1991). The impact of temperature on structural organization is well recognized in thermodynamic research spanning fields, including thermal concentrator models (Xia *et al*., 2025). Thermo-acoustic properties show similar temperature-driven effects. Variations in concentration and temperature significantly influence the distribution of charges within molecules, and these changes also affect the nature of interactions (e.g., H-bonding, dipole-dipole, ion-dipole, etc.) (Devi *et al*., 2021).

The present work is based upon previously reported studies (Jamal *et al*., 2021; Jamal *et al*., 2015). In the current research, the densities, p, and sound velocities, u, of solutions of Na-NAP in varying concentrations of aqueous D-mannitol (5 wt.%, 7 wt.%, 9 wt.%, and 10 wt.%) were reported over the temperature range (293.15-313.15K). The temperature range was chosen to reflect storage, processing, and physiological conditions relevant to pharmaceutical formulations. The acquired experimental results were used to compute the apparent and partial molar volume ($\emptyset_v$, $\emptyset_v^\circ$), transfer partial volume($\Delta_{tr}\emptyset_{v)}^\circ$), partial molar isentropic compressibility ($\emptyset_k^\circ$). In addition to volumetric and acoustic studies, density functional theory (DFT) calculations were used to accompany the experimental findings. A computational study provides molecular-level insight into the stability, electronic properties, and the role of hydrogen bonding in governing the association between the drug and D-mannitol. From such properties, important information about drug solvation, bioavailability, structural stability, conformational dynamics, and intermolecular interactions can be obtained.

## MATERIALS AND METHODS

### *Materials*

The details of the chemicals used are provided in table 1. The chemical structures of Na-NAP and D-mannitol are shown in fig. S1. These compounds were used without any additional purification, except for drying in a desiccator to prevent absorption of $CO_2$ or moisture.

### *Solution preparation*

Deionized, distilled, and degassed water with a conductivity of $<10^{-6}$ S/cm was used to prepare solutions. By contrasting experimental $\boldsymbol{\rho}$ and $\boldsymbol{u}$ data with published values from the literature in table S1, the purity of water was also assessed. The compounds were weighed employing a Sartorius GC 2102 analytical balance with an accuracy of ±0.0001 mg. The solutions were prepared in glass vials and sealed with aluminum foil to prevent moisture and $CO_2$ contamination.

### *Density and sound velocity measurements*

The calibration of DSA-5000M was carried out by using air and deionized water before measuring the $\rho$ and $u$ of solutions (Paar, 2011). $\boldsymbol{\rho}$ and the $\boldsymbol{u}$ of Na-NAP in aqueous D-mannitol system were measured by using a density sound velocity meter (DSA-5000M) at various temperatures (293.15-313.15K) and atmospheric pressure. The two cells make up the dual-purpose device: a density cell and a sound velocity cell. With an accuracy of ±0.01 K, the temperature of both cells is stabilized by an integrated Peltier thermostat (PT-100). The DSA-5000 M measures density up to 3 g/cm$^3$ and sound velocity between 1000 and 2000 m/s at a temperature range of T = 273.15 to 343.15 K (Jamal *et al*., 2017). The uncertainties in measuring the T, $u$, and $\rho$ of DSA 5000 M are found to be $\pm 10^2$ K, ±0.029 m/s, and $\pm 1\times10^{-6}$ g/cm$^3$, respectively.

## RESULTS

### *Apparent and partial molar volume*

The $\rho$ values of the investigated system of Na-NAP with water and in aqueous solutions of different concentrations of D-mannitol were measured at temperatures ( 293.15 - 313.15 K) with intervals of 5K, and the acquired values are indicated in table S2.

Equation 1 was used to compute the apparent molar volume($\emptyset_v$) using the density data and results have been presented in the form of plots in fig.1 (Millero *et al*., 1978).

$$\emptyset_v = \frac{1000(p^0-p)}{mpp^0} + \frac{M}{p} \quad (1)$$

Where $m$, $\emptyset_v$, $p^0$, M, and $p$ are the molality, apparent molar volume, pure solvent's density, molar mass of investigated solute, and density of solution, respectively. Fig S2 illustrates the variation in experimental density with the concentrations of both the drug and the sweeteners in the studied solution at variable temperatures and atmospheric pressure. The values of partial molar volume ($\emptyset_v^\circ$) has been obtained using Masson's equation 2 and least square fit technique have been mentioned in table 2 (Millero, 2014).

$$\emptyset_{v=}\emptyset_v^\circ + S_v\sqrt{m} \quad (2)$$

### *Expansibility and Hepler's constant*

Temperature affects the volumetric properties and equation 3 indicates the sensitivity of $\emptyset_v^\circ$ to temperature (Lomesh *et al*., 2024)

$$\emptyset_v^\circ = a_1 + a_2T + a_3T^2 \quad (3)$$

Here, T represents the temperature in Kelvin, and the values of the coefficients. $a_1$, $a_2$, and $a_3$ that were determined by the procedure of elimination using equation 3. Expansibility $\emptyset_E^\circ$ is a parameter that is acquired from the

derivation of $\emptyset_v^\circ$ in relation to temperature at constant pressure as shown in equation 4 (Ryshetti *et al*., 2015), and obtained data illustrated in table 2. Hepler's derived the second derivative of partial molar volume $\left(\frac{\partial^2 \emptyset_v^\circ}{\partial T^2}\right)$ by using equation 5 to determine the ability of solute to form and break the structure within the solutions.

$$\emptyset_E^\circ = \frac{\partial \emptyset_v^\circ}{\partial T} = a_2 + 2a_3 T \quad (4)$$

$$\left(\frac{\partial E_\emptyset^\circ}{\partial T}\right) = \left(\frac{\partial^2 \emptyset_v^\circ}{\partial T^2}\right) = 2a_3 \quad (5)$$

The expansibility ($\emptyset_E^\circ$) and partial molar volumes ($\emptyset_v^\circ$) are used to derive isobaric thermal expansion coefficients ($\alpha$) at various temperatures and constant pressure by employing equation 6 (Omar *et al*., 2018).

$$\alpha^\circ = \frac{\emptyset_E^\circ}{\emptyset_v^\circ} \quad (6)$$

***Transfer partial molar volume***

The concept of transfer partial molar volume is frequently employed to assess the effect of cosolvent and cosolute on solute solvent interactions. The sign and magnitude of $\Delta_{tr}\emptyset_v^\circ$ offer important information on the nature of interactions in interacting moieties. Equation 7 has been used to compute the transfer partial molar volume. (Banipal *et al*., 2001).

$$\Delta_{tr}\emptyset_v^\circ = \emptyset_{v\,(in\ aqueoues\ \ D-mannitol\ solution)}^\circ - \emptyset_{v\,(in\ water)}^\circ \quad (7)$$

***Apparent and partial molar isentropic compressibility***

The $\emptyset_k$, for Na-Nap in water and in aqueous D-mannitol solution over the temperature range (293.15–318.15) K with 5K intervals at atmospheric pressure, has been calculated from the measured values of *u* using equation 8 (Rajagopal and Gladson, 2011).

$$\emptyset_k = \frac{1000(\beta_s\rho^\circ - \beta_s^\circ\rho)}{m\rho\rho^\circ} + \frac{\beta_s.M}{\rho} \quad (8)$$

The density of pure solvents is $\rho^\circ$, $\rho$ denotes the density of solutions, and $M$ is the molar mass, $m$ is the concentration of Na-NAP in molality, $\beta_s^\circ$ is the isentropic compression of the solvent. $\beta_s$, which was computed using $\rho$ and $u$ data in equation 9, represents the isentropic compression for the studied solutions.

$$\beta_s = [\rho u^2]^{-1} \quad (9)$$

The data are fitted to the following well-known equation 10, since a linear relationship has been found between drug concentration and $\emptyset k$, and the same trend is observed across all concentrations.

$$\emptyset_k = \emptyset_k^\circ + S_k\sqrt{m} \quad (10)$$

***Theoretical studies***

DFT-based quantum chemical simulations were used to confirm the molecular interactions in gas and aqueous environments. The single point energy, molecular electrostatic potential (MEP) surface and optimization of the molecule were calculated using density functional theory (DFT) with functional RB3LYP and 6.311++G (2d, 3p) basis set. The Polarised Continuum Model scrf (I-PCM, solvent = water) was used to account for the solvent effect. The Gaussian 16 application module default parameters were used for optimization. In addition, the dipole moment, HOMO-LUMO and global reactivity descriptor in both the gas and aqueous phases were estimated and represented in fig. 2. Non covalent interaction (NCI) analysis carried out to confirm the interaction and plot is represented in fig.3.

***Global reactivity descriptor***

The parameters proposed by Koopman's theorem (Bellafont *et al*., 2015; Tsuneda *et al*., 2010) for global reactivity, include the electrophilicity index (ω), chemical potential (μ), hardness (η), electronegativity (χ) and softness (S). These values are calculated from the molecular orbital energies ($E_H$ and $E_L$).

## DISCUSSION

The density of drug solutions increases with increasing D-mannitol concentration. The -OH groups of D-mannitol provide the drug molecules with advantageous binding sites, enabling tighter molecular packing. The density of the solution of sodium naproxen in aqueous D-mannitol is higher than that of pure water, enhancing the system's compactness. It indicates that solutions have a higher degree of intermolecular interactions. Additionally, drug molecules bind to more distinct regions in solution when D-mannitol is present. As a result, compactness increases, increasing the drug's density in an aqueous solution of D-mannitol (Ayranci and Sahin, 2008; Galán *et al*., 2003). On the other hand, as the temperature rises, the density decreases because solute-solvent interactions are disrupted, intermolecular binding forces weaken, and molecular mobility increases. The solution density decreases at high temperatures due to this loss of compactness. An increase in temperature increases the thermal energy, which raises the dynamic energy of molecules in solution, thereby surpassing their binding energy and lowering the solution density (Negadi *et al*., 2017). Similarly, strong attractive interactions, primarily caused by hydrogen bonding and hydration phenomena, are reflected in the higher values $\emptyset_v$ with increasing D-mannitol concentration. The same trend is observed for all concentrations. From a structural perspective, D-mannitol is a polyhydroxy carbohydrate with several -OH groups that can form hydrogen bonds, whereas sodium naproxen has a hydrophobic aromatic component along with polar groups ($-COO^-$ and $-OCH_3$). In solution, the medication is stabilized by the complementary interactions between these functional groups. The temperature and D-mannitol content both raise the apparent molar volume of sodium naproxen. The increased solvation of sodium naproxen in the aqueous D-mannitol solution and improved solute–solvent interactions are responsible for this phenomenon. Table S3 shows that $\emptyset_v$ values increase with increasing temperature. Solute-solvent interaction indicates that D-

mannitol improves sodium naproxen's stability and solubility. Bioavailability and oral absorption are directly affected by improved solubility. The release of water molecules from the weakly bound solvation shell allows solute and solvent molecules to approach more closely at elevated temperatures, supporting the observed volume changes. Integrating pertinent studies from the recent literature has led to a more thorough comparative understanding of these findings (Leguizamón *et al*., 2011; Lomesh, Bala, and Nathan, 2019; Lomesh *et al*., 2024; Zafarani-Moattar and Shekaari, 2005). Positive value of $\left(\frac{\partial^2 \emptyset_v^\circ}{\partial T^2}\right)$ indicates structure making nature of solute, when Hepler's constant is negative, the solute acts as a structure breaker (Mohapatra *et al*., 2025). The current study indicates the structure-making behaviour of Na-NAP in both water and an aqueous solution of D-mannitol. This behaviour is compatible with improved stability and reduced compressibility, both of which are important for enhancing formulation performance.

The isobaric thermal expansion coefficient is also used to interpret the solute-solvent interactions (Cabani *et al*., 1976). As the temperature rises, the values of $\alpha^\circ$ for Na-NAP in the aqueous solutions of D-mannitol increases, suggesting a weakening of binding between Na-NAP and water.

The data of $\Delta_{tr}\emptyset_v^\circ$ is positive and gradually rises, indicating that solute-cosolute interactions prevail over solute-solvent interactions (Nain, 2019). Polar/ionic sites $(Na^+, COO^-)$ of Na-NAP and several -OH groups of D-mannitol have the potential to interact and form a strong hydrogen bond. The $Na^+$cation may coordinate with the lone pair of oxygen of -OH groups of D-mannitol, the $COO^-$ group of Na-NAP may interact with the hydroxyl group of D-mannitol. Such interactions promote the formation of complex hydration structures and weaken the electrostriction effect. The order of interaction changes with the increasing concentration. D-mannitol creates a stabilizing, hydrophilic environment, while fewer water molecules are firmly bound to Na-NAP. Since of the favourable solute–cosolute interactions, the positive transfer partial volume in this case can be taken as an indication of decreased electrostriction and improved structural ordering. A structural examination of Na-NAP and D-mannitol reveals that the following natures of molecular interactions are possible.

- Ion-hydrophilic interactions in the $(Na^+, COO^-)$ groups of Na-NAP and $(-OH)$ groups of D-mannitol.
- Hydrophilic-hydrophilic interactions among the polar part of Na-NAP and the polar part of D-mannitol.
- Hydrogen bonding in $(-OH)$ of D-mannitol and $(-OCH_3, -COO^-)$of Na-NAP molecules.
- Hydrophobic-hydrophobic interactions in the non-polar group of Na-NAP molecules and side chain $(-CH_3)$ of d-mannitol molecules.

The positive values of $\Delta_{tr}\emptyset_v^\circ$ for a mixture of Na-NAP with D-mannitol in aqueous solutions elaborated by the Friedman and Krishnan's co-sphere overlap model (Streng and Wen, 1974). According to the overlapping model, an overlap occurs when two or more molecules come into contact in solution. Consequently, it causes a change in the thermodynamic properties of the molecules, i.e., a change in the transfer partial volume (Lin *et al*., 2006). Data in table 3 show that as the concentration of D-mannitol in an aqueous solution increases, D-mannitol molecules gradually replace solvent molecules (water), leading to an increase in the transfer partial volume, which indicates stronger interactions between the solute and cosolute. The cosphere overlap model reveals that ion-hydrophilic and hydrophilic-hydrophilic interactions contribute positively to the $\Delta_{tr}\emptyset_v^\circ$ values while interactions between ions and hydrophobic molecules negatively contribute (Devi *et al*., 2021; Lamba *et al*., 2023). In the current investigations, the positive values of $\Delta_{tr}\emptyset_v^\circ$ illustrate that the dominant interaction is ion-hydrophilic, hydrophilic-hydrophilic, and hydrogen bonding, as shown in fig. S3. The positive transfer partial volumes suggest that the solute promotes solvent network expansion, indicating strong hydrophilic contacts. This result is compatible with increased solubility and beneficial molecular packing, which are crucial for enhancing formulation performance.

Sound velocity (*u)* for studied solution has been measured and reported in supplementary information, table S4. The ***u*** data for the investigated solutions increased with increasing concentrations of Na-NAP and D-mannitol at temperatures between 293.15 and 313.15 K, in 5 K intervals. The molecules of water around the solute molecule lead to the interactions of solute-solvent in an aqueous solution of Na-NAP. The solvent molecule is replaced when D-mannitol is added as a cosolute to an aqueous solution of the drug. As a result, the system becomes more compact. The reason for the higher sound velocity of aqueous solution of D-mannitol is that the more compact structure of solutions at higher concentrations of D-mannitol (Barthel, 1954).

The effect of concentration of solute and cosolute on $\emptyset$ is depicted in fig.S4. The results in table 4 show that solvent molecules surrounding the ionic groups of the solute are less compressible than those in the bulk solution. Stronger hydration shells, associated with reduced partial molar compressibility at higher temperatures, may affect the drug's mobility and association in aqueous media, which in turn may influence its distribution properties. As D-mannitol concentration rises, the apparent molar isentropic compressibility rises as well, confirming the presence of interactions between solute-cosolute (hydrophilic-hydrophilic), as indicated in table S5. The key reason behind the rise in $\emptyset_k$ with temperature is the increase in discharge of water molecules from the hydration shell of Na-NAP into bulk water (Reis, 1998).

**Table 1**: Specification and purity of studied compounds.

| Name of chemicals | Molecular weight g/mol | Source | CAS No. | Purity of mass fraction |
|---|---|---|---|---|
| Sodium Naproxen | 252.25 | Alfa Aesar | 22204-53-1 | ≥99.25% |
| D-Mannitol | 182.17 | Sigma-Aldrich | 69-65-8 | ≥99% |

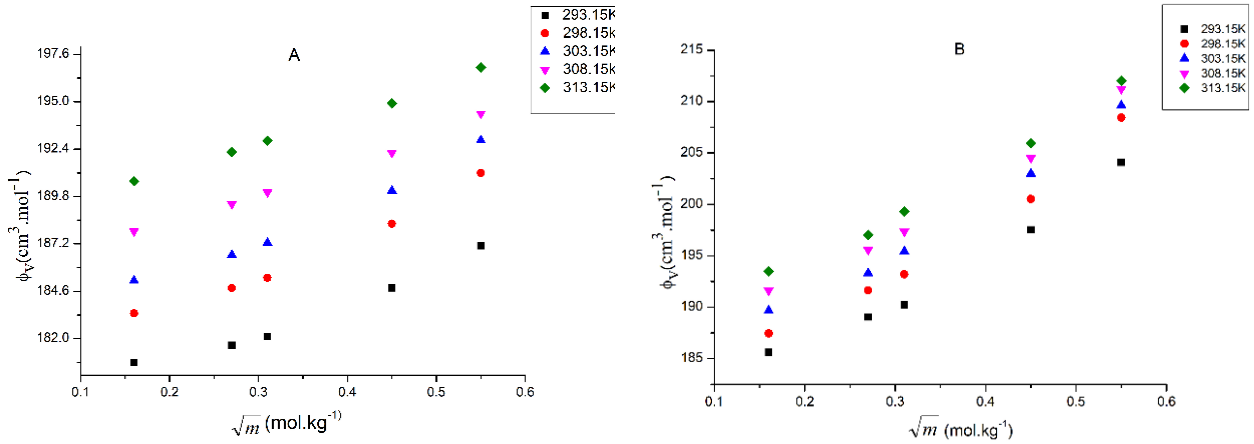


**Fig. 1**: Plots of apparent molar volume ($\emptyset_v$) vs molality (m) of (A) sodium naproxen in water, (B) 5% D-mannitol, illustrating molecular interactions

**Table 2**: Partial molar volume ($\emptyset_v^\circ$) of sodium naproxen (Na-NAP) in water and different concentrations of D-mannitol (%w/w) at T= (293.15K-313.15K) and atmospheric pressure, illustrating structure making behaviour

| D-mannitol W/W % | T(K) | ($\emptyset_v^\circ$) (cm$^3$ mol$^{-1}$) | $\emptyset_E^\circ$ (cm$^3$ mol$^{-1}$ K$^{-1}$) | $\alpha^0$ x10$^{-3}$(K) | $\left(\frac{\partial^2\emptyset_v^\circ}{\partial T^2}\right)_p$ (cm$^6$ mol$^{-2}$K$^{-1}$) |
|---|---|---|---|---|---|
| | 293.15 | 180.39 | 0.362 | 2.004 | |
| | 298.15 | 182.67 | 0.381 | 2.083 | 0.0038 |
| 0 | 303.15 | 184.32 | 0.401 | 2.168 | |
| | 308.15 | 186.35 | 0.419 | 2.246 | |
| | 313.15 | 188.78 | 0.438 | 2.318 | |
| | 293.15 | 183.68 | 0.238 | 1.299 | |
| | 298.15 | 185.14 | 0.263 | 1.418 | 0.0048 |
| 5 | 303.15 | 186.30 | 0.287 | 1.538 | |
| | 308.15 | 188.23 | 0.311 | 1.650 | |
| | 313.15 | 189.73 | 0.334 | 1.763 | |
| | 293.15 | 187.15 | 0.373 | 1.995 | |
| | 298.15 | 188.32 | 0.408 | 2.169 | 0.0070 |
| 7 | 303.15 | 190.96 | 0.443 | 2.310 | |
| | 308.15 | 193.04 | 0.478 | 2.478 | |
| | 313.15 | 196.11 | 0.513 | 2.618 | |
| | 293.15 | 194.63 | 0.405 | 1.845 | |
| | 298.15 | 196.10 | 0.422 | 2.030 | 0.0078 |
| 9 | 303.15 | 198.09 | 0.439 | 2.207 | |
| | 308.15 | 201.26 | 0.456 | 2.366 | |
| | 313.15 | 202.83 | 0.473 | 2.540 | |
| | 293.15 | 194.75 | 0.470 | 2.413 | |
| | 298.15 | 197.69 | 0.483 | 2.443 | 0.0026 |
| 10 | 303.15 | 199.91 | 0.496 | 2.481 | |
| | 308.15 | 202.46 | 0.509 | 2.514 | |
| | 313.15 | 205.46 | 0.522 | 2.540 | |

**Table 3**: Values of transfer partial molar volume ($\Delta_{tr}\emptyset_v^\circ$) for Na-NAP in aqueous and different concentrations of D-mannitol (%w/w) at T= (293.15K-313.15K) and atmospheric pressure.

| $\Delta_{tr}\emptyset_v^\circ$ ($cm^3$/mol) | | | | | |
|---|---|---|---|---|---|
| D-mannitol (%w/w) | 293.15K | 298.15K | 303.15K | 308.15K | 313.15K |
| 5 | 3.29 | 2.47 | 1.98 | 1.88 | 0.95 |
| 7 | 6.76 | 5.65 | 6.64 | 6.69 | 7.33 |
| 9 | 14.29 | 13.43 | 13.77 | 14.91 | 14.05 |
| 10 | 14.36 | 15.02 | 15.59 | 16.11 | 16.69 |

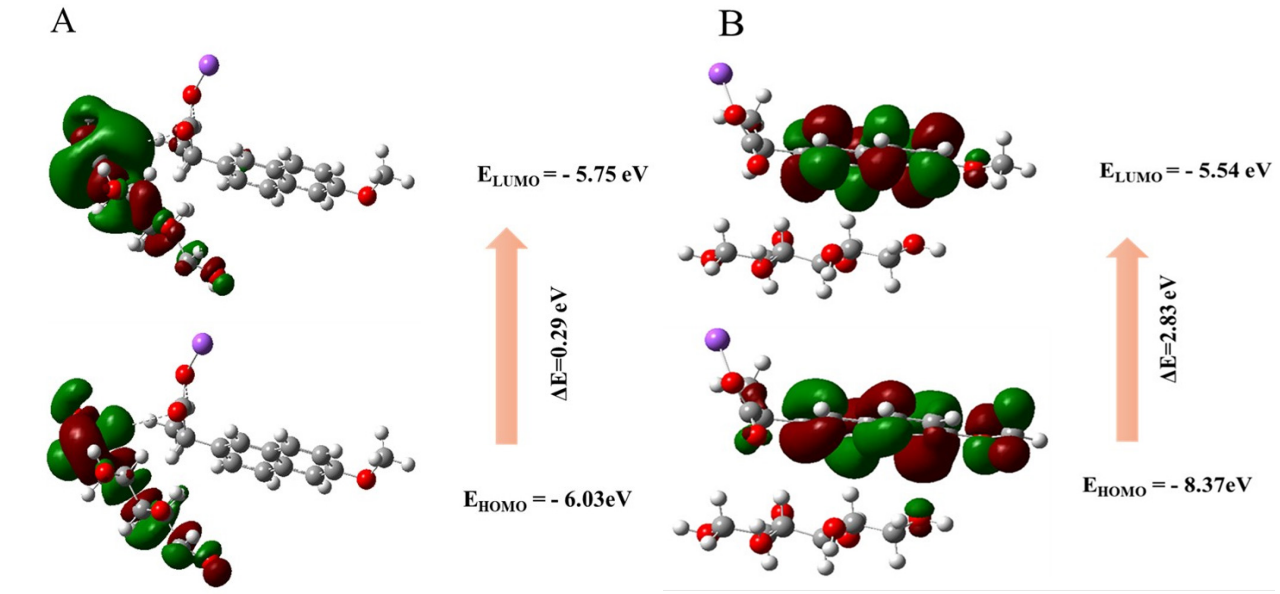


**Fig. 2**: HOMO-LUMO representation of (A) $Complex_{(gas)}$ and (B) $Complex_{(aqueous)}$ with enhanced stability in aqueous phase.

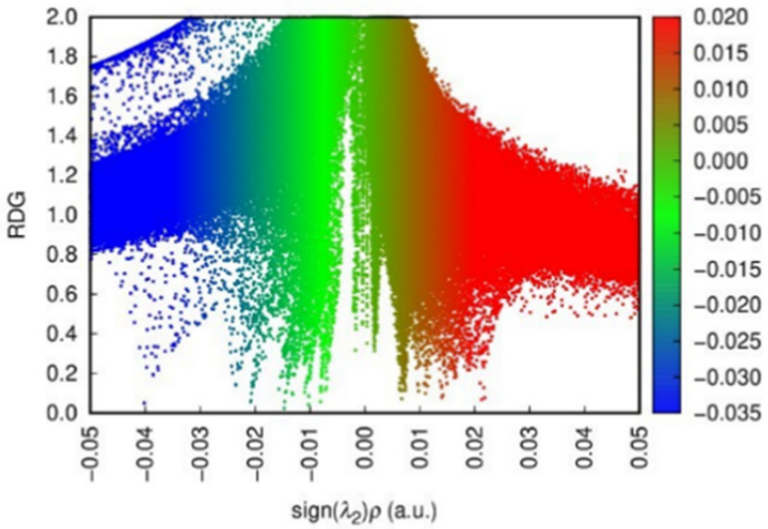


**Fig. 3**: RDG vs sign ($\lambda_2$) $\rho$ plot of Na-NAP and D-mannitol complex, blue region indicating the hydrogen bonding potential.

**Table 4**: The partial molar isentropic compressibility ($\emptyset_k^\circ$) of sodium naproxen (Na-NAP) in water and different concentrations of aqueous D-mannitol (%w/w) at T= (293.15-313.15K) and atmospheric pressure, indicating enhanced molecular ordering.

| $\emptyset_k^\circ \times 10^{-4}(cm^3/mol\ Pa)$ | | | | | |
|---|---|---|---|---|---|
| D-mannitol (%w/w) | 293.15 K | 298.15 K | 303.15 K | 308.15 K | 313.15 K |
| 0 | -12.27 | -11.08 | -9.19 | -8.66 | -8.36 |
| 5 | -9.34 | -8.66 | -7.64 | -7.21 | -6.64 |
| 7 | -10.47 | -10.24 | -9.79 | -9.25 | -8.66 |
| 9 | -9.11 | -8.18 | -8.11 | -7.92 | -7.80 |

**Table 5**: Calculated $E_{HOMO}$, $E_{LUMO}$, energy gap ($E_L$–$E_H$), electronegativity (χ), hardness (η), chemical potential (μ), softness (S) and electrophilicity index (ω).

| System | D (Debye) | $E_L$ eV | $E_H$ eV | $E_{(L-H)}$ eV | χ eV | μ eV | η eV | ω eV | S $eVs^{-1}$ |
|---|---|---|---|---|---|---|---|---|---|
| Na- NAP(g) | 10.47 | -6.15 | -9.00 | 2.85 | 7.57 | -7.57 | 1.42 | 40.88 | 0.71 |
| Na-NAP(aq) | 14.35 | -5.60 | -8.50 | 2.90 | 7.05 | -7.05 | 1.45 | 36.03 | 0.73 |
| D-mannitol(g) | 3.74 | -2.80 | -5.05 | 2.25 | 3.92 | -3.92 | 1.13 | 8.67 | 0.56 |
| D-mannitol(aq) | 4.50 | -2.76 | -5.11 | 2.35 | 3.93 | -3.93 | 1.18 | 9.10 | 0.59 |
| Complex(gas) | 10.26 | -5.74 | -6.03 | 0.29 | 5.89 | -5.89 | 0.14 | 2.43 | 0.07 |
| Complex(aq) | 11.18 | -5.54 | -8.37 | 2.83 | 6.96 | -6.96 | 1.42 | 34.22 | 0.71 |

The obtained energy values (Hartrees) of the optimized structure of Na-NAP and D-mannitol in gas and aqueous phase are $Na\text{-}NAP_{(gas)}$ (-929.542), $Na\text{-}NAP_{(aqueous)}$ (-929.638), $D\text{-}mannitol_{(gas)}$ (-687.695), $D\text{-}mannitol_{(aqueous)}$ (-679.6159), $complex_{(gas)}$-1670.40, and $complex_{(aqueous)}$ -1618.75. The dipole moments were calculated at the same level. The dipole moment of all systems in aqueous solution is larger than in the gas phase. It is predicted that as the solvent's polarity increases, the dipole moment rises (Frank, 1935). The electronic structure is strongly influenced by solvation effects in the aqueous phase, driven by hydrogen bonding and electrostatic interactions between water molecules and the solute (Targema *et al*., 2013). In the aqueous phase, the DFT results clearly distinguish the contributions of electrostatic forces, hydrogen bonding, and hydration-shell interactions to the stabilization of the drug-D-mannitol system. Charge distributions and dipole moment values reflect electrostatic interactions (Singh *et al*., 2024) indicating a strong coulombic attraction between the drug's negatively charged carboxylate groups and the polar -OH groups of D-mannitol. The reduced HOMO-LUMO gap, negative energy values, and NCI plots with significant blue-green sections all support hydrogen-bonding contributions and confirm directional H-bonding between solute pairs.

Furthermore, hydration-shell interactions are evident in single-point energy calculations in the aqueous phase, indicating greater stability upon solvation (Mazumdar *et al*., 2023). The stability of the complex was further strengthened by van der Waals interactions close to its aromatic ring. The structure-making behaviour seen in the experimental section is caused by solute-solute interactions, which are confirmed to be the main stabilizing factor. Visualization of the distribution of charge in the molecule observed from the band gap ($\Delta E_{L\text{-}H}$) of the title compounds in the gas and aqueous phase, and the obtained values are specified in table 5. Fig S5 indicates that $\Delta E_{L\text{-}H}$ for both compounds in the aqueous phase is greater than the gaseous phase, indicating that it is more stable in the aqueous phase. The NCI analysis of the complex in confirmed the potential for hydrogen bonding, as evidenced by a large blue zone surrounding its hydroxyl groups.

Blue (hydrogen bonding) and green (van der Waals) patches were intensely concentrated between Na-NAP and D-mannitol in the complex's NCI plot in fig. S6, as opposed to between each molecule and the surrounding medium. The hydroxyl groups of mannitol and the carboxylate group of Na-NAP were found to interact prominently, forming numerous hydrogen bonds that are crucial to the system's stability.

The Quantification of ω requires positive values of μ and η, which indicate energy stabilization when the system receives a charge from the surrounding molecule. The existence of high or low values of μ and ω shows the electrophilic or nucleophilic behavior of the molecules (Liu and Parr, 1997). Hardness and softness correlate with molecular stability. In molecules with a narrow HOMO–LUMO gap, reactivity increases, and vice versa (Frank, 1935). As the complex moved towards greater chemical stability in the aqueous phase, its hardness increased from 0.14 eV (gas) to 1.42 eV (aqueous), and its softness decreased from 2.43 eV (gas) to 34.22 eV (aqueous). The complex's electrophilicity (ω), a measurement of the molecule's capacity to take electrons, became significantly increased. It illustrates that the complex becomes a much more potent electron acceptor in water, suggesting a more conductive environment for molecular interactions and potentially increased biological significance.

## CONCLUSION

In the current study, thermos-acoustic parameters of Na-NAP in an aqueous solution of D-mannitol were analysed across a range of temperatures. The $\emptyset_v^\circ$ and $\emptyset_k^\circ$ have been computed and analysed in terms of molecular interactions. Positive partial molar volumes and increasing trends with increasing D-mannitol concentration suggest strong solute–solute interactions. Strong drug-excipient interactions, which favour a more expanded solvation structure, are reflected in the obtained positive transfer partial volumes, indicating efficient molecular compatibility in aqueous conditions. Hepler's constant with a positive sign further confirmed the structure-making behaviour of the Na-NAP. Computational studies involving HOMO–LUMO analysis, dipole moment, and global reactivity descriptors supported the experimental observations by highlighting the stability, reactivity and polar nature of the interacting species. The HOMO-LUMO distributions and global reactivity descriptors indicate strong electronic interactions that promote hydrogen bonding and solute-solvent organization, consistent with the observed structure-forming behaviour. The NCI examination clearly indicates significant hydrogen bonding, which contributes to positive transfer partial volumes and a lower isentropic compressibility. High dipole moments help sustain the hydration shell by linking molecular polarity to volumetric and acoustic factors observed experimentally. These descriptors have the potential to serve as the foundation of data-driven formulation design methodologies, connecting fundamental thermo-acoustic behaviour to practical formulation performance. As a result, the experimental findings not only contribute to molecular understanding but also align with current efforts to merge experimental and computational approaches to optimize drug-excipient compatibility, improve formulation stability, and elucidate drug-biomolecule interactions at the molecular level.

***Acknowledgments***
The authors are thankful to the authorities for providing the facilities to conduct the research.

***Authors' contributions***
Sumaira Shoukat: Performed experimental work and wrote manuscript; Muhammad Asghar Jamal: Supervised experimental design and contributed to manuscript revision; Faiz Ahmed: Carried out density functional theory (DFT) study. Majid Muneer: Contributed to review and editing. All authors reviewed and approved the final manuscript.

***Funding***
There was no funding.

***Data availability statement***
The datasets generated during and/or analysed during the current study are available from the corresponding author on reasonable request.

***Ethical approval***
Not applicable.

***Conflict of interest***
The corresponding author, on behalf of all co-authors, declares that there is no conflict of interest related to this study.

***Supplementary data***
https://www.pjps.pk/uploads/2026/04/SUP1776701238.pdf

## REFERENCES

Ayranci E and Sahin M (2008). Interactions of polyethylene glycols with water studied by measurements of density and sound velocity. *JCT*, **40**(8): 1200-1207.

Banipal TS, Singh G and Lark BS (2001). Partial molar volumes of transfer of some amino acids from water to aqueous glycerol solutions at 25 C. *J. Solut. Chem*, **30**: 657-670.

Barthel R (1954). Sound velocity in some aqueous solutions as a function of concentration and temperature. *JASA,* **26**(2): 227-230.

Bellafont NP, Illas F and Bagus PS (2015). Validation of Koopmans' theorem for density functional theory binding energies. *PCCP*, **17**(6): 4015-4019.

Cabani S, Conti G and Matteoli E (1976). Partial molal expansibilities of organic compounds in aqueous solution. I. Alcohols and ethers. *J. Solut. Chem,* **5**: 751-763.

Chen Y, Yang C, Mao J, Li H, Ding J and Zhou W (2019). Spermine modified polymeric micelles with pH-sensitive drug release for targeted and enhanced antitumor therapy. *RSC advances*, **9**(20): 11026-11037.

Devi S, Kumar M, Sawhney N, Syal U, Sharma AK and Sharma M (2021). Volumetric, acoustic and viscometric studies of L-histidine and L-serine in aqueous levofloxacin solutions at different temperatures and concentrations. *JCT*, **154**, 106321.

Dudley MN (1991). Pharmacodynamics and pharmacokinetics of antibiotics with special reference to the fluoroquinolones. *Am. J. Med,* **91**(6): S45-S50.

Filippa MA and Gasull EI (2014). Experimental determination of Naproxen solubility in organic solvents and aqueous binary mixtures: Interactions and thermodynamic parameters relating to the solvation process. *J. Mol. Liq,* **198**: 78-83.

Frank FC (1935). Dipole induction and the solvent effect in dipole moment measurements. *Proc. R. Soc. Lond. A Math. Phys. Sci,* **152**(875): 171-196.

Galan JJ, Del Castillo J, Gonzalez-Perez A, Czapkiewicz J and Rodriguez JR (2003). Density and sound velocity studies of aqueous solutions of tetradecyltrimethylammonium nitrate at different temperatures. *J. Solut. Chem,* **32**: 919-927.

Jamal MA, Fatima J, Naseem B, Muneer M and Ibrahim M (2021). Molecular interaction studies of antidepressant drug with aqueous caffeine using volumetric and acoustic methods. *J. Mol. Liq*, **329**: 115525.

Jamal MA, Khosa MK, Muneer M, Saif MJ, Bhatti HN, Naz S and Javed J (2015). Acoustical behavior of some amino acids in aqueous disodium citrate solutions over temperature range (298.15-313.15) K. *PJPS,* **28**(5): 1613-1618.

Jamal MA, Naseem B, Khosa MK, Muneer M and Khan JH (2017). Effect of anionic micellar medium on thermo-acoustical parameters of aspartic acid and serine solutions. *J. Mol. Liq*, **237**: 14-22.

Jiang X, Zhu C and Ma Y (2013). Density and viscosity of sorbitol/maltitol in L-ascorbic acid aqueous solutions at T=(293.15 to 323.15) K. *J. Mol. Liq*, **188**: 67-73.

Kumar H, Sharma R, Kumar V and Alothman AA (2021). Exploration of the solvation behavior of the synthesized 1-hexyl-3-methylimidazolium bromide [C6mim][Br] ionic liquid with L-cysteine and N-acetyl L-cysteine) in aqueous medium at different temperatures. *J. Mol.Liq*, **324**: 114664.

Lamba M, Chakraborty N, Juglan KC, Singla M and Sharma R (2023). Volumetric-acoustic study of disodium ethylenediaminetetraacetic acid with propylene and hexylene glycol at different temperatures. *J. Mol. Liq*, **390**: 123045.

Leguizamon ARH, Delgado DR, Martinez MAR and Martinez F (2011). Apparent molar volumes of sodium naproxen in water at several concentrations and temperatures. *Lat. Am. J. Pharm*, **30**(3): 619-623.

Li Y, Li YH, Wang FA and Ren BZ (2013). Densities and viscosities of cefodizime sodium in water and normal saline from (278.15 to 313.15) K. *Thermochim. Acta*, **568**: 189-195.

Lin G, Bian P and Lin R (2006). The limiting partial molar volume and transfer partial molar volume of glycylglycine in aqueous sodium halide solutions at 298.15 K and 308.15 K. *JCT*, **38**(2): 144-151.

Liu S and Parr RG (1997). Second-order density-functional description of molecules and chemical changes. *J. Chem. Phys,* **106**(13): 5578-5586.

Lomesh SK, Bala M, Kumar D and Kumar I (2019). Investigation of molecular interactions of the drug Diclofenac Sodium Salt in water and aqueous sorbitol systems at different temperatures (305.15 K–315.15 K). *J. Mol. Liq,* **289**: 109479.

Lomesh SK, Bala M and Nathan V (2024). A study of enhancing the solubility of streptomycin sulphate in sorbitol using volumetric, acoustic and viscometric properties. *J. Mol. Liq,* **404**: 124997.

Mazumdar P, Kashyap A and Choudhury D (2023). Investigation of hydrogen bonding in small nucleobases using DFT, AIM, NCI and NBO technique. *Comput. Theor. Chem*, **1226**: 114188.

Millero FJ (2014). Estimation of the partial molar volumes of ions in mixed electrolyte solutions using the Pitzer equations. *J. Solut. Chem,* **43**: 1448-1465.

Millero FJ, Lo Surdo A and Shin C (1978). The apparent molal volumes and adiabatic compressibilities of aqueous amino acids at 25. degree. *J. Phys. Chem*, **82**(7): 784-792.

Mohapatra P, Panda S, Mishra D, Singh S and Talukdar M (2025). Interference of potassium chloride and diammonium hydrogen phosphate on volumetric, viscometric and spectroscopic properties of aqueous nicotinamide. *RSC advances*, **15**(3): 1813-1830.

Nain AK (2019). Volumetric, acoustic and viscometric studies of solute-solute and solute-solvent interactions of isoniazid in aqueous-glucose/sucrose solutions at temperatures from 293.15 K to 318.15 K. *JCT*, **133**: 123-134.

Naseem B, Khan M and Jamal MA (2016). Acoustical studies of pharmaceutical excipients in binary solvent mixtures. *J. Mol. Liq*, **220**: 581-591.

Naseem B, Mukhtar M, Arif I and Jamal MA (2017). Effect of concentration and temperature on the interactions between saline soil salts and nitro phosphate fertilizer under atmospheric pressure: A thermo-acoustic approach. *J. Mol. Liq*, **247**: 151-163.

Negadi L, Feddal-Benabed B, Bahadur I, Saab J, Zaoui-Djelloul-Daouadji M, Ramjugernath D and Negadi A (2017). Effect of temperature on density, sound velocity, and their derived properties for the binary systems glycerol with water or alcohols. *JCT,* **109**: 124-136.

Omar QM, Jaubert JN and Awan JA (2018). Densities, apparent molar volume, expansivities, Hepler's constant, and isobaric thermal expansion coefficients of the binary mixtures of piperazine with water, methanol, and acetone at T= 293.15 to 328.15 K. *Int. J. Chem. Eng*, **2018**(1): 8689534.

Paar A (2011). Instruction manual:"Tribology measuring cell T-PTD200 ". *Anton Paar*.

Perlovich GL, Kurkov SV, Kinchin AN and Bauer-Brandl A (2004). Thermodynamics of solutions III: Comparison of the solvation of (+)-naproxen with other NSAIDs. *Eur. J. Pharm. Biopharm*, **57**(2): 411-420.

Rajagopal K and Gladson SE (2011). Interactions of potassium fluoride with coexistent components in water–dimethyl sulfoxide mixed solvent at different temperatures. *Thermochim. Acta*, **525**(1-2): 197-205.

Reis JCR (1998). New thermodynamic relations concerning apparent molar isentropic compression and apparent and partial isentropic compressibilities. *J. Chem. Soc. Faraday Trans,* **94**(16): 2385-2388.

Ryshetti S, Gardas RL and Tangeda SJ (2015). Effect of temperature on solvation behaviour of diclofenac sodium salt in aqueous glycine and l-proline solutions. *JCT*, **82**: 125-133.

Sajid TA, Jamal MA, Saeed M and Muneer M (2021). Elucidation of molecular interactions between amino acid and imidazolium based ionic liquid in an aqueous

system: volumetric and acoustic studies. *J. Mol. Liq*, **335**: 116513.

Shahazidy U, Jamal MA, Muneer M, Naseem B and Qureshi AK (2022). Elucidation of molecular interactions between sugar alcohol and dimethyl sulfoxide in aqueous system: Volumetric and acoustic study. *J. Mol. Liq*, **350**: 118543.

Shahazidy U, Jamal MA, Naseem B and Asghar H (2024). Physicochemical and sweetness behavior of kosmotropic and chaotropic ions in aqueous solutions of polyhydroxy compound. *Food Chem*, **432**: 137216.

Sharma SK, Nathan V, Kumar D and Kishore K (2017). Molecular interaction studies of antibiotic drug Doxycycline Hyclate with aqueous mannitol using volumetric and acoustic methods. *J. Mol. Liq*, **231**: 647-654.

Singh MB, Jain P, Mohammad F, Singh P, Bahadur, I., and Abedigamba, O. P. (2024). Significant increase in the dipole moment of graphene on functionalization: DFT calculations and molecular dynamics simulations. *ACS omega*, **9**(14): 16458-16468.

Streng WH and Wen WY (1974). Calculation of Gurney parameters for aqueous tetraalkylammonium halides based on Friedman's cosphere-overlap model. *J. Solut. Chem*, **3**: 865-880.

Targema M, Obi-Egbedi NO and Adeoye MD (2013). Molecular structure and solvent effects on the dipole moments and polarizabilities of some aniline derivatives. *Comput. theor. Chem*, **1012**: 47-53.

Tsuneda T, Song JW, Suzuki S and Hirao K (2010). On Koopmans' theorem in density functional theory. *JCP*, **133**(17):

Warminska D (2012). Volumetric and acoustic properties of D-mannitol in aqueous sodium or magnesium chloride solutions over temperature range of 293.15–313.15 K. *Carbohydr. Res*, **349**: 44-51.

Xia G, He X, Jia Y, Zhu Y and Tian Z (2025). Design of a cylindrical thermal rotary concentrator based on transformation thermodynamics. *Materials*, **18**(19): 4440.

Zafarani-Moattar MT and Shekaari H (2005). Apparent molar volume and isentropic compressibility of ionic liquid 1-butyl-3-methylimidazolium bromide in water, methanol and ethanol at T=(298.15 to 318.15) K. *JCT,* **37**(10): 1029-1035.